

Study of Structural and Electronic Properties of Rutile Titanium Dioxide (TiO₂) Using Density Functional Theory (DFT)

Basima Farzam

Department of General Technical and Professional Subjects, Faculty of Engineering, Faryab University, Maymana, Faryab 1801, AFGHANISTAN

Corresponding Author: basimfarzam@gmail.com



www.jrasb.com || Vol. 4 No. 1 (2025): February Issue

Received: 16-01-2025

Revised: 26-01-2025

Accepted: 01-02-2025

ABSTRACT

The study aims to investigate the structural and electronic properties of Rutile TiO₂ due to its wide range of applications, and is a promising material for the mass market for low-cost, high-efficiency and optic-electronic devices because of its outstanding properties, inherent n-type conductivity, low toxicity, and availability[1]. All these modern applications call for better understanding of its properties, but there is a lack of investigation on the structural, electronic and elastic properties of R-TiO₂ using LDA exchange-correlation function[2]. In this project, band structure, the density of state, and structural optimizations of rutile titanium dioxide were studied and analysed using the Quantum-Espresso package and LDA exchange-correlation function[3], [4]. By performing this calculation, the estimated lattice parameter 'a' for rutile titanium dioxide using LDA method is 4.5653 Å and 'c' is 3.1422 Å, which are relatively close to experimental results which are 4.593 Å and 2.9 Å. Also, According to the results, rutile titanium dioxide (R-TiO₂) has a direct band gap semiconducting property with an energy gap of 1.50 eV using LDA exchange correlation function.

Keywords- Rutile titanium dioxide, LDA exchange-correlation function, Density functional theory (DFT).

I. INTRODUCTION

Recently the Titanium dioxide has been the subject of theoretical and experimental studies from decades, because of its unique properties[5],[6]. It has good photocatalytic activity and a high dielectric constant with a wide range of electrical conductivity[7]. Here are three common polymorphs of TiO₂ namely; (i) rutile phase with a tetragonal, space group of P4₂/mnm and E_g ~ 3.05 eV, (ii) anatase phase with a tetragonal space group of I4₁/amd and E_g ~ 3.23 eV and (iii) brookite phase with a band gap of E_g ~ 3.26 eV[9].

Crystal parameters are a = 4.594 Å, c = 2.959 Å for rutile, a = 3.785 Å, c = 9.514 Å for anatase and a = 5.456 Å, b = 9.182 Å, c = 5.143 Å for brookite[10]. Between all these three polymorphs of TiO₂, the rutile is the most stable phase of TiO₂ and has a wide range of application due its unique properties, such as high refractive index, stability at a high temperature[11].

Also, the rutile phase have gotten more attention than the anatase and brookite due its key characteristics, including the optical property and electrical bandgap[12]. The Brookite and Anatase phases have been extensively studied compared to the Rutile phase. This may be because it is computationally expensive due to the number of atoms in its unit cell and its difficulty in preparation[10]. Some of its important properties, for instance the structural and electronic properties are still under deliberation. As a result, more investigation into rutile phase properties is needed to understand its potential uses better. Following this introductory we describe computational approach and the DFT method. We present and discuss electronic energies and related properties of rutile TiO₂, as obtained by our self-consistent solution of the relevant system of equations defining the local density approximation (LDA). We compare our findings to previous, corresponding theoretical and experimental ones. Finally, we summarize our results.

II. METHODOLOGY

The Quantum Espresso algorithm was used to do the structural optimization and electronic calculation utilizing the density functional theory-supported plane wave pseudopotential approach[13]. Pseudopotential (PP) is utilized to model the electron-ion interaction while the electron-electron interaction is modeled with the help of the local density approximation (LDA)[14]. For the exchange-correlation interaction, LDA method has been employed. This exchange-correlations was chosen because no adjustable parameter was required hence computationally efficient. Plane wave method was used to represent electronic wave function. Crystal structures were relaxed at $T=0\text{K}$ and $P=0\text{ GPa}$ and convergence tests were carried out. After doing convergence tests, the cutoff energy of 200 eV was selected.

Then, all of the provided computations are done utilizing this optimized structure. In addition, all the calculations were done using Quantum Espresso package. First of all, structural optimization was run with *x* driver and self consistent calculation was run with *scf* driver to get the electron density. Also, the band structure calculation was run with *bands.x*. In order to generate more data the post processing tool was run with *pp.x* driver. In addition, by using the Quantum Espresso package the parameters, such as; the Brillouin zone grid, crystal systems, the kinetic cut-off energy, and the lattice, was quantified in an input file, with kinetic energy cut-off as well as different convergence thresholds for the selfconsistent field used till suitable values are obtained. Lattice parameters of R-TiO₂ were obtained in two steps. In the first step, the convergence calculations of the total energy were performed using different kpoints generated with the method of Monkhorst and Pack[15]. The MonkhorstPack grid is a standard technique for collecting samples from the Brillouin zone (Monkhorst and pak 1976)[16]. The accuracy of the convergence is totally reliant on the integration grid selected. The Monkhorst-Pack approach provides for both accurate integration of parts in the Brillouin zone, as well as sampling on the whole Brillouin zone[17]. Different k-point samplings were used for convergence test for the unit cell. Energy difference for the unit cell change was less than 0.0001 eV when the k-point grid was $12 \times 12 \times 3$. This energy did not change further when I increased the k-point grid. This procedure was used for LDA method. In the second step, we tested the evolution of the total energy as a function of the lattice constant for R-TiO₂. Similarly, to get optimum value for cut-off energy, the cut-off energy was ranged from 50 eV to 200 eV. The energy was converged at cut-off 200 Ry, so all the calculations were done by applying this optimized value (200 Ry) for cutoff energy. During the process of optimizing the lattice parameters, experimental lattice parameter values were taken into account as the starting point[18]. The

Birch-Murnaghan equation of state was used to fit the data, and the lowest value of the fitted curve was used to determine the required lattice constant[12]. To get the highest possible value for the plane wave cut-off energies, the cut-off energy was increased from 50 Ry to 200 Ry after checking that the lattice parameters plus k-point meshes were created to their ideal values. When there was no longer any area for the energy to be changed, the perfect values were found. Given that every system aims to be in a low-energy state, this was a very important point (ground state). In addition, the Xcrysden tool was used to visualize the crystal structures of R-TiO₂. Also, for band structure calculation the k-points grid is most important parameter for LDA method[19]. In this particular piece of work, the building of the specific k-points was achieved by the use of the Monkhorst-Pack approach[20]. When calculating the band structures of the systems, Kokač and Čausà found that it was necessary to take into account the points and pathways with a high degree of symmetry that were created by the Xcrysden software[21]. In order to get more insight of band structure the total density of state (TDOS) and partial density of state (PDOS) using LDA XC functional was plotted using orignine tool.

III. RESULT AND DISCUSSION

3.1 Structural Optimization

Geometrical relaxation is the first stage in any first-principles calculation to eliminate a certain amount of uncertainty to accurately forecast other values such as the electronic bandgap and elastic characteristics. Geometry optimization is a computational procedure in which atomic coordinates and cell parameters are modified so that the structure's total energy is minimized and a stable system is obtained[24]. A stable geometry will result from all optimization techniques. When the atoms in each optimal geometrical structure are relaxed and possibly stable, they will feel no forces or stress. As a result, full geometry optimizations of TiO₂ structures were carried out. Tetragonal rutile TiO₂ with lattice parameters $a=b \neq c$, $\alpha=\beta=\gamma=90^\circ$ is the system being studied[25].

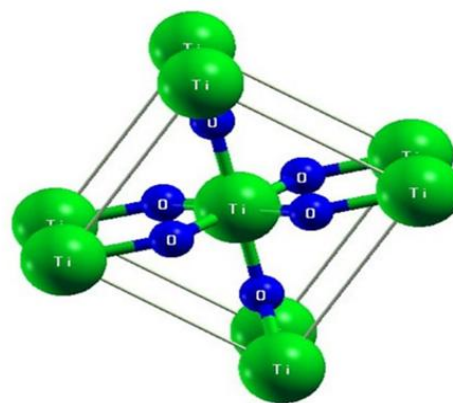


Figure 1: Optimized structures for rutile TiO₂.

Table 1 shows the TiO₂ lattice constants from the DFT-LDA and the related experimental results. To avoid specific errors and obtain correct results for structural and electronic properties, the optimized lattice parameters of a and c, as shown in table (1), are used for this calculation.

Table 1: Calculated Lattice Parameters of R-TiO₂

Bulk TiO ₂	XC	a (Å)	c (Å)	Ref.
R-TiO ₂	LDA	4.653	3.1422	Present work
R-TiO ₂	Experiment	4.5938	2.9586	[26]

The computed lattice parameter 'a' for TiO₂ using LDA-PZ is 'a' 4.653 and 'c' 3.1422, whereas the published experimental value for TiO₂ is 4.5938 and

2.9586[26], [27]. Consequently, it was established that LDA-PZ represents the materials' features more accurately. According to the findings of this comparative study, the choice of XC functional has a significant influence on the ground-state properties of materials. The determined bond angles for TiO₂ using LDA-PZ are 131.94° and 90.00°, which are on average identical to the experimental and other LDA functional values from table 2. In general, it was discovered that, while LDA functional is inadequate at expressing the electrical characteristics of these confined orbitals, it does a great job of characterizing the energy of the system and accurately replicating the structural features[28]. By relaxing the TiO₂ structure's atomic locations and lattice characteristics, ground state simulations were conducted, and then lattice parameters were then compared to experimental results.

Table 2: Bond Angles and Bond Lengths for R-TiO₂

	R-TiO ₂ (Bond lengths Å)		R-TiO ₂ (Bond angles A°)	
	Present work (DFT)	Ti-O	1.96	Ti-O-Ti-O
DFT [29]	Ti-O	1.85	Ti-O-Ti-O	131.92° 90.00°
Experiment work [30]	Ti-O	1.95	Ti-O-Ti O-Ti-O	130.97° 90.00°

3.2 Electronic properties

It is generally acknowledged that DOS and electronic band structure play key roles in establishing crystal structure[26]. Fundamentally, the categorization of materials, especially metals, semiconductors, and insulators, depends on a system's electronic characteristics. The size and presence of the energy band gap between the conduction band and the valence band determine the kind of material.

The electronic are Fig. 2 illustrate the electrical band structures of bulk TiO₂ estimated using LDA exchange correlations and pseudopotential. Regardless of whether exchange correlations or pseudopotentials are

utilized, the computed band gap is underestimated compared to the experimental value. TiO₂'s empirically observed bandgap is 3.0 eV; our computational estimates show band gaps ranging from 1.54 eV to 2.53 eV. The band gap using LDA exchange correlation is 1.54. The conduction band minimum at -point and the conduction band minimum at R and M are almost equal, according to our estimates of the electronic band structure. This degeneration is present in all exchange correlations and pseudopotentials[29]. We concluded that various bulk TiO₂ band configurations did not predict the band gap nor the norm-conserving pseudopotential.

Table 3: Calculated Energy Band Gap of TiO₂

compound	XC	Bandgap (eV)	Ref
R-TiO ₂	LDA	1.54	Present work
R-TiO ₂	LDA	1.5	[2]
R-TiO ₂	Experiment work	3.03	[30]

In addition, for TiO₂, our calculation result is 1.54 eV for direct band gap using LDA which is pretty close to other LDA values, certifying the reliability of our methods. As a result the obtained result shows that, the LDA exchange-correlation is a good method for determining TiO₂'s band structure. The Projected density of states (PDOS) is depicted in Fig. 2 using LDA. In the

DOS analysis method, we set the Fermi levels to 0 eV to enable comparability[30]. Based on our calculations, we also found nonzero Ti-PDOS in the valence band and nonzero O-PDOS in the conduction band close to the Fermi level. These nonzero PDOS values imply a substantial hybridization between Ti atoms' 3d orbitals and O atoms' 2p orbitals. In addition, we discovered two

different peaks in the PDOS of the Ti3d orbital, showing a clear split into sub-bands. The sub-band separation of the 3d orbital of Ti atoms is discussed in the crystal-field theory of transition-metal (di) oxide complexes. Such d-states are divided by crystal field theory into three-fold degenerate t_{2g}-like d_{xy}, d_{yz}, and d_{xz} type states and two fold-degenerate e_g-like states with and character. Furthermore, for the range of R-TiO₂ from -6 to -0.55, the density of state of R-TiO₂ is classified into three groups of occupied and unoccupied states, separated by gaps, using LDA exchange-correlation.

The O 2p and Ti 3d of O and Ti atoms contribute the most to the R-TiO₂ from -6 to -0.55. Second, no states exist between 0.55 and 0.93. Finally, O 2p and Ti 3d states contribute to total DOS from an energy range of 0.966 to 2.988 eV. Our analyses indicated that the best strategy to explain the electrical structure of TiO₂ other functional materials is to use a mix of LDA and pseudopotential [26].

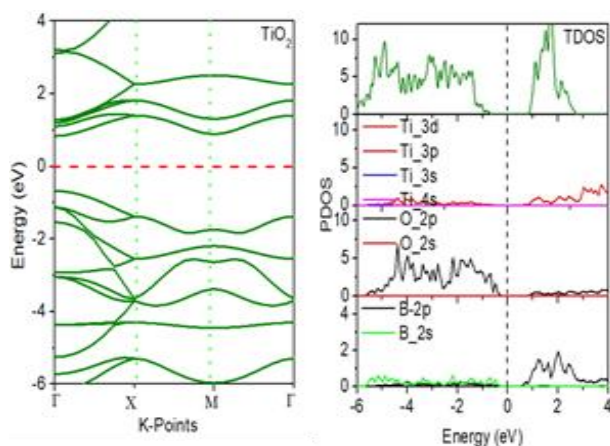


Figure 2: Electronic Band Structures and T-DOS of TiO₂, Using LDA Exchange-correlation

IV. CONCLUSION

This paper presents the findings of first-principles analyses of the structural, electrical, and elastic characteristics of TiO₂'s Rutile phase. The Quantum Espresso algorithm was used to do the structural optimization and electronic calculation utilizing the density functional theory-supported plane wave pseudopotential approach. The estimated lattice parameter 'a' for rutile titanium dioxide using LDA method is 4.5653 Å and 'c' is 3.1422 Å, which are relatively close to experimental results which are 4.593 Å and 2.9 Å. The Rutile structure was discovered to have a small band gap of 1.54 eV using the LDA exchange-correlation function which is in good accord with the experimental values and previous LDA based calculations. This shows significant improvement compared to other theoretical calculations[2]. The k-points of 12×12×3 were used for band structure calculation.

REFERENCES

- [1] H. Tian, F. Xin, X. Tan, and W. Han, "High lithium electroactivity of boron-doped hierarchical rutile submicrosphere TiO₂," *J. Mater. Chem. A*, vol. 2, no. 27, pp. 10599–10606, 2014, doi: 10.1039/c4ta01438c.
- [2] M. Radecka, "Structural properties of TiO₂ nanomaterials," *J. Mol. Struct.*, 2017, doi: 10.1016/j.molstruc.2017.12.064.
- [3] M. S. Waghmode, A. B. Gunjal, J. A. Mulla, N. N. Patil, and N. N. Nawani, "Studies on the titanium dioxide nanoparticles: biosynthesis, applications and remediation," *SN Appl. Sci.*, vol. 1, no. 4, pp. 1–9, 2019, doi: 10.1007/s42452-019-0337-3.
- [4] G. Giuliani and G. Vignale, "Density functional theory," *Quantum Theory Electron Liq.*, pp. 327–404, 2010, doi: 10.1017/cbo9780511619915.008.
- [5] V. I. Lakshmanan, A. Bhowmick, and M. Abdul Halim, "Titanium dioxide: Production, properties and applications," *Titan. Dioxide Chem. Prop. Appl. Environ. Eff.*, no. June, pp. 75–130, 2014.
- [6] J. R. Chelikowsky, "Structural and Electronic Properties of Titanium Dioxide," no. January, 2014, doi: 10.1103/PhysRevB.46.1284.
- [7] A. Soussi et al., "Electronic and Optical Properties of TiO₂ Thin Films: Combined Experimental Electronic and Optical Properties of TiO₂ Thin Films: Combined Experimental and Theoretical Study," *J. Electron. Mater.* no. May, 2021, doi: 10.1007/s11664-021-08976-8.
- [8] A. Soussi et al., "Electronic and optical properties of TiO₂ thin films: combined experimental and theoretical study," *J. Electron. Mater.*, vol. 50, no. 8, pp. 4497–4510, 2021.
- [9] "Literature review."
- [10] T. Mahmood, C. Cao, W. S. Khan, Z. Usman, F. K. Butt, and S. Hussain, "Electronic, elastic, optical properties of rutile TiO₂ under pressure: A DFT study," vol. 407, pp. 958–965, 2012, doi: 10.1016/j.physb.2011.12.114.
- [11] M. Jankulovska, "Study of the electrochemical properties of nanostructured TiO₂ electrodes," no. July 2015.
- [12] H. Zhang, J. F. Ban, and X. Di, "Structural Characteristics and Mechanical and Thermodynamic Properties of Nanocrystalline TiO₂," 2014.
- [13] I. A. González Ramirez, L. A. Alcalá Varilla, and J. A. Montoya, "A DFT study about the effects of exchange-correlation functional on the structural and electronic properties of Anatase," *J. Phys. Conf. Ser.*, vol. 1219, no. 1, 2019, doi: 10.1088/1742-6596/1219/1/012019.

- [14] E. Grabowska, A. Zaleska, J. W. Sobczak, M. Gazda, and J. Hupka, "Boron-doped TiO₂: Characteristics and photoactivity under visible light," *Procedia Chem.*, vol. 1, no. 2, pp. 1553–1559, 2009, doi: 10.1016/j.proche.2009.11.003.
- [15] M. H. Samat, N. Adnan, M. F. M. Taib, O. H. Hassan, M. Z. A. Yahya, and A. M. M. Ali, "Structural Electronic and Optical properties study of Brookite TiO₂," *Solid State Sci. Technol.*, vol. 24, no. 2, pp. 107–120, 2016.
- [16] A. Gupta and A. Thakur, "An Overview On Structural, Morphological And Optical Properties Of Titanium – Dioxide Nanoparticles," vol. 07, no. 07, pp. 2815–2818, 2020.
- [17] N. Dharmale, S. Chaudhury, R. Mahamune, and D. Dash, "Comparative study on structural , electronic , optical and mechanical properties of normal and high pressure phases titanium dioxide using DFT Comparative study on structural , electronic , optical and mechanical properties of normal and high pressure pha," 2020.
- [18] "Structural and optical characterization of the crystalline phase transformation of electrospinning TiO₂ nanofibres by high temperatures annealing," vol. 65, no. October, pp. 459–467, 2019.
- [19] R. José Pérez Menéndez, "Fiber-Optic Ring Resonator Interferometer," *Interferom. - Recent Dev. Contemp. Appl.*, pp. 1–22, 2019, doi: 10.5772/intechopen.80569.
- [20] A. Fahmi, C. Minot, B. Silvi, and M. Causa, "Theoretical analysis of the structures of titanium dioxide crystals," *Phys. Rev. B*, vol. 47, no. 18, p. 11717, 1993.
- [21] E. Ekuma and D. Bagayoko, "Ab-initio Electronic and Structural Properties of Rutile Titanium Dioxide," pp. 1–25.
- [22] J. Muscat, V. Swamy, and N. M. Harrison, "First-principles calculations of the phase stability of TiO₂," *Phys. Rev. B*, vol. 65, no. 22, p. 224112, 2002.
- [23] S. Jensen and D. Kilin, "Anatase (100) thin film surface computational model for photoelectrochemical cell," *Int. J. Quantum Chem.*, vol. 112, no. 24, pp. 3874–3878, 2012.
- [24] G. Copper et al., "First-Principles Study on the Elastic Mechanical Properties and," 2022.
- [25] P. Filippatos, N. Kelaidis, M. Vasilopoulou, D. Davazoglou, and A. Chroneos, "applied sciences Structural, Electronic, and Optical Properties of Group 6 Doped Anatase TiO₂ : A Theoretical Approach," 2021.
- [26] M. M. M. Mikami, S. N. S. Nakamura, O. K. O. Kitao, H. A. H. Arakawa, and X. G. X. Gonze, "First-principles study of titanium dioxide: rutile and anatase," *Jpn. J. Appl. Phys.*, vol. 39, no. 8B, p. L847, 2000.
- [27] H. Chen, X. Li, R. Wan, S. Kao-walter, and Y. Lei, "A DFT study of the electronic structures and optical properties of (Cr , C)," *Chem. Phys.*, 2017, doi: 10.1016/j.chemphys.2017.11.021.
- [28] D. Yu, W. Zhou, Y. Liu, B. Zhou, and P. Wu, "Density functional theory study of the structural , electronic and optical properties of C-doped anatase TiO₂ (101) surface," *Phys. Lett. A*, vol. 379, no. 28–29, pp. 1666–1670, 2015, doi: 10.1016/j.physleta.2015.04.044.
- [29] D. Ziental et al., "Titanium Dioxide Nanoparticles : Prospects and Applications in Medicine."
- [30] M. K. Butt et al., "A DFT study of structural, magnetic, elastic and optoelectronic properties of lanthanide based XAlO₃ (X=Nd, Gd) compounds," *J. Mater. Res. Technol.*, vol. 9, no. 6, pp. 16488–16496, 2020, doi: <https://doi.org/10.1016/j.jmrt.2020.11.055>.